Observing co-seismic displacements using 1-Hz data from a network of reference stations: a comparison of different data processing methods

Michail Gianniou
National Cadastre and Mapping Agency S.A.
Mesogion Ave. 288, 15562 Athens, Greece

Abstract

GPS data recorded at 1 Hz at stations of the Hellenic Positioning System (HEPOS) are processed to detect co-seismic displacements. Two different data processing methods are tested: geodetic relative positioning in kinematic mode and Precise Point Positioning (PPP). A strong earthquake (Mw=6.4) which occurred in western Greece near Andravida on 8 June 2008 is used to compare the two approaches. Co-seismic coordinate variations of up to 69 mm (peak to peak) and coordinate rates of up to 45 mm/s have been estimated.

For baselines ranging between 67 and 118 km in length the two tested methods were found to be equivalent regarding their ability to detect horizontal displacements, whereas PPP proved to be more sensitive in detecting vertical displacements. For the effective estimation of the arrival time of the surface seismic waves at a station we propose the computation of station velocities. Furthermore, station velocities proved to be suitable for the determination of the duration of the dynamic displacements at a station.

Keywords: *Co-seismic displacements; 1-Hz GPS data; Precise Point Positioning; HEPOS.*

1. Introduction

The Hellenic Positioning System (HEPOS) in an RTK-network consisting of 98 permanent GPS reference stations distributed throughout Greece. The Hellenic National Cadastre and Mapping Agency (NCMA S.A., former KTIMATOLOGIO S.A.) developed HEPOS in order to modernize the geodetic infrastructure in Greece and, thus, to facilitate the establishment of the Hellenic Cadastre. In each RTK-network it is of particular importance that the coordinates of the reference stations are known with accuracy in the order of 1 cm. This requirement is a great challenge for HEPOS, due to the strong geodynamic effects taking place in Greece. As known, Greece is the seismo-tectonically most active area in Europe (Hollenstein, 2006). The intense tectonic activity has a considerable impact on the coordinates of the reference stations. For this reason, data from the HEPOS network are regularly analyzed at NCMA S.A. in order to detect and estimate the tectonic movements. The analysis of data collected since the beginning of the operation of HEPOS yielded a detailed velocity field over Greece (Gianniou, 2010a). In addition, permanent displacements that occurred as a result of strong earthquakes have been detected and quantified (Gianniou, 2010b).

The above mentioned results have been derived from daily solutions obtained by processing 15-seconds GPS measurements in static mode. Using 1-Hz GPS data surface seismic waves can be detected. Several approaches for the data processing have been reported in the literature. Genrich and Bock (1992) computed kinematic solutions using the integer carrier phase ambiguities resolved from static solutions. Bock et al. (2000) and Nikolaidis et al. (2001) utilized single-epoch ambiguity resolution, while other researchers used Precise Point Positioning (PPP) solutions (Kouba, 2003a; Takasu, 2006; Yusaku, 2008). In this work we computed kinematic solutions using two different post-processing methods, i.e. PPP and geodetic relative positioning. This article describes the processing schemes and compares the results of the two approaches.

2. Available data

During the first years of the operation of HEPOS, several strong earthquakes (ML>6.0) with different characteristics took place in certain areas of Greece. Fig.1 gives the epicenters of the four most severe events occurred in 2008 and 2009. Their local magnitudes vary between 5.6 and 6.5, whereas their focal depths range between 25 km and 56 km (www.gein.noa.gr).

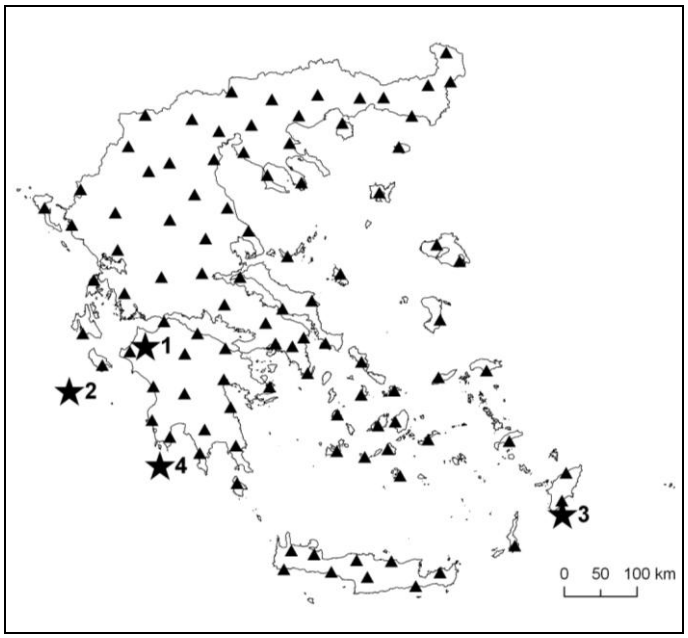

Fig. 1. Epicenters of the earthquakes (stars) and HEPOS stations (triangles).

The Andravida earthquake (star 1 in Fig. 1), that occurred on 8 June 2008 at 12:25:27 GMT, is the strongest (Mw=6.4) and the shallowest (25 km) of the four events. Moreover, unlike the other events, its epicenter is surrounded by HEPOS reference stations. So, multiple PPP and baseline solutions involving different stations can be computed. For these reasons, this seismic event has been chosen for comparing the PPP and baseline solutions.

The Andravida earthquake is one of the largest strike-slip earthquakes occurred in western Greece during the last decades (Ganas et al., 2008). Surface rupture of the fault has not been reported but landslides (mostly rockfalls), liquefaction, coastal subsidence, and settlement of fills have been widely observed within approximately 15 km of the fault (Margaris et al., 2008). GPS data analysis revealed permanent displacements of about 1 cm at nearby permanent reference stations (Ganas et al., 2008; Gianniou, 2010b).

3. Processing schemes

As mentioned in section 1 we computed kinematic solutions using two different post-processing approaches, namely PPP and geodetic relative positioning in kinematic mode. The baseline solutions were calculated using TRACK ver. 1.27, the kinematic module of GAMIT software package (Herring et al., 2010). The PPP computations were made using GrafNav ver. 8.40, a software that is particularly suitable for kinematic processing. GrafNav computes kinematic baselines and PPP solutions using Kalman filter algorithms and takes advantage of precise ephemerides, satellites clock errors and differential code biases (DCB) information (Novatel, 2011).

For the PPP solutions dual frequency phase observations were used together with IGS final orbits (sp3 files) and clocks (RINEX clock files) (Kouba, 2003b). The satellite clock information was available every 30 sec, a rate that ensures accurate PPP solutions (Kouba, 2003a). The default

elevation mask in the software is 7.5 degrees. For evaluation purposes higher elevation cut-off angles up to 10 degrees have been tested using the data of this study. The tests showed that the higher elevation masks have a minor positive effect on the horizontal coordinates but a considerably stronger negative effect on the estimation of the heights. For this reason all PPP computations were made using an elevation mask of 7.5 degrees. The tropospheric zenith delay was modeled as a state in the Kalman filter. Phase ambiguities are not fixed in PPP, but are instead left to converge as floating point values.

In the case of baseline solutions the ambiguities were fixed to integer values. The elevation mask for the baseline processing was set to 10 degrees, which is the default value within TRACK software. The MTT mapping function and seasonal model were used. As in the case of PPP, Precise orbits were used. The selection of the stations forming the kinematic baselines was of particular importance. TRACK computes the relative position of one or more stations with respect to a fixed station. To ensure the highest possible accuracy in the determination of the baseline components, the baseline length has to be minimized, i.e. the base station should be as close as possible to the station that will be investigated for displacements (station 030A in our case, see Fig. 2). On the other hand, the closest station (012A in our example) is also in motion during the event and so the variation in the baseline length represents the relative motion between the two stations and not the actual movement of the rover. In order to select the base station we first computed the PPP solutions for all surrounding stations to find the closest station to the epicenter that is not affected by the earthquake. The results are given in the following.

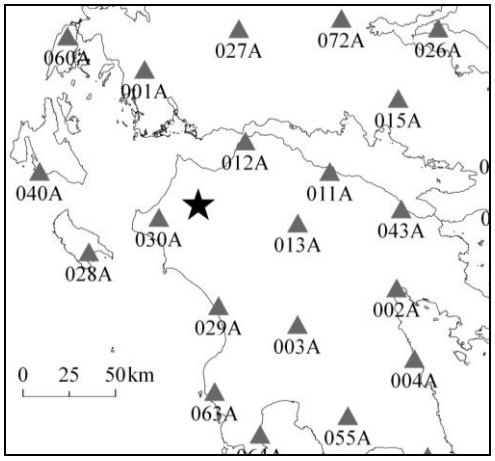

Fig. 2. Epicenter of the Andravida earthquake (star) and next HEPOS stations (triangles). The distances between the stations and the epicenter are: 23 km (030A), 43 km (012A), 55 km (013A), 65 km (028A) and 79 km (001A).

4. Data analysis - results

All HEPOS stations are equipped with Trimble NetRS receivers and Trimble Geodetic antennas with spherical domes. The 1-Hz HEPOS data are stored in hourly RINEX files. Processing tests using one hour of data led to a high number of unresolved phase ambiguities in the baseline solutions, while two hours of observations yield good results. In addition, the use of two-hour data improves the accuracy of the PPP solution (Novatel, 2008). For these reasons we used two hours of observations (11:00-13:00 GPS time) both for the PPP and the baseline solutions. The geodetic frame for the GPS data processing was ITRF2005. The estimated ECEF ITRF2005 coordinates were afterwards transformed to local NEU coordinates for the evaluation of the displacements and the velocities of the stations. The results are shown in Fig. 3 to Fig. 10, where the time is expressed relative to the Andravida earthquake (12:25:27 GMT), the East-North coordinates are given relative to their mean values for the interval 12:00-13:00 and the curves are shifted for clarity.

4.1 PPP results

Stations 030A, 012A, 013A, 028A and 001A (Fig. 2) have been chosen to compute PPP solutions. Fig. 3 shows the East of stations 030A and 012A as computed from the PPP solution. The intense variations around 12:26 indicate the earthquake. Having a more detailed look at the time-series around the time of the event (Fig. 4) the arrival of the surface seismic wave can be clearly identified. The first considerable variation in the position of station 030A is observed 14 sec after the event, where North changes 21 mm. The first motion at station 012A is observed 20 sec after the event, where East changes 51 mm. Although the arrival of the seismic waves can be clearly detected, the duration of the displacements can hardly be assessed due to the noise of the time-series. To ensure a straightforward estimation of the movements we estimated station velocities by differentiating the coordinates obtained from the PPP solutions. Fig. 5 gives the velocities (North component) for the five stations under investigation. Comparing the North values for stations 030A and 012A (Fig. 4) to the corresponding velocities (Fig. 5) it becomes obvious that using the velocities, the arrival of the seismic waves is made easier to detect and the duration of the displacements can be more accurately estimated. Examining Fig. 5 we can detect motion at station 030A up to approximately 220 sec after the event, whereas the corresponding duration for station 012A is about 190 sec. It is furthermore noteworthy that small motions can be observed at stations 013A and 028A. At station 001A (which is the most distant from the epicenter) the arrival of the surface seismic wave is not obvious. Only weak indications are given by the time-series of East and North (not shown here for the sake of brevity). However, those indications are not strong enough to draw conclusions with certainty about the arrival of the seismic waves at station 001A.

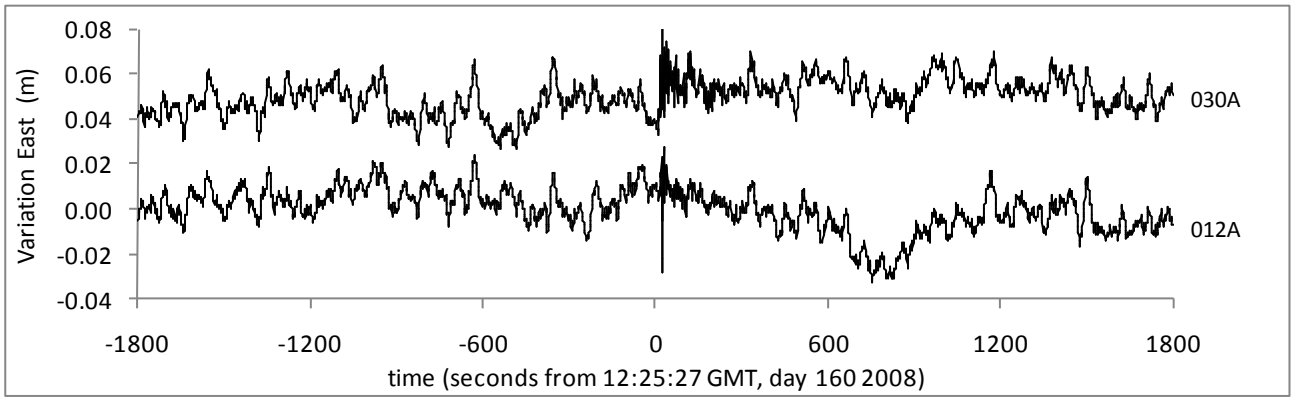

Fig. 3. Time-series (11:55 - 12:55) of East of stations 030A and 012A estimated by the PPP solution.

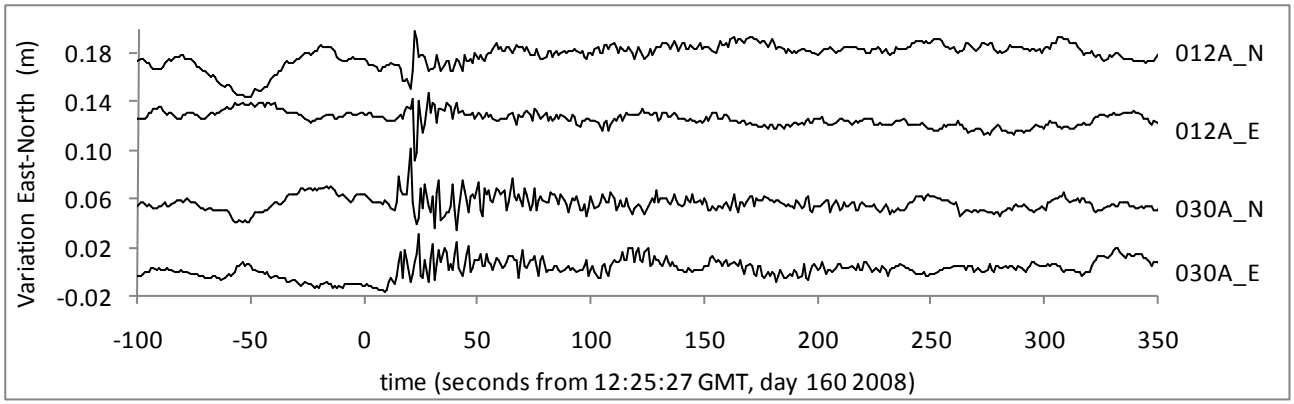

Fig. 4. Time-series (12:23 - 12:31) of East and North of stations 030A and 012A estimated by the PPP solution.

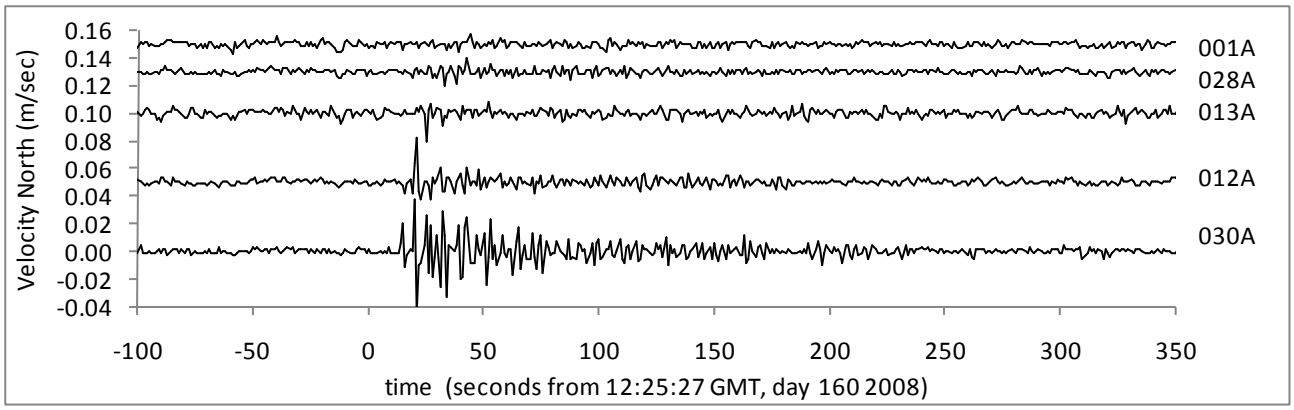

Fig. 5. Time-series (12:23 - 12:31) of stations' velocities (North component) obtained from the PPP solution.

Due to the significantly higher noise level in the height estimation, the threshold for the detection of vertical motion is considerably bigger than in the case of horizontal motion. Nevertheless, vertical displacements have been detected at two sites. Fig. 6 shows the estimated velocities (Up component) for stations 030A, 012A and 028A. Vertical velocities up to 2.7 cm/sec and 1.4 cm/sec are detectable at stations 030A and 012A, respectively. At station 028A no vertical motion can be detected. This is also the case for stations 013A and 001A that are not shown in Fig. 6.

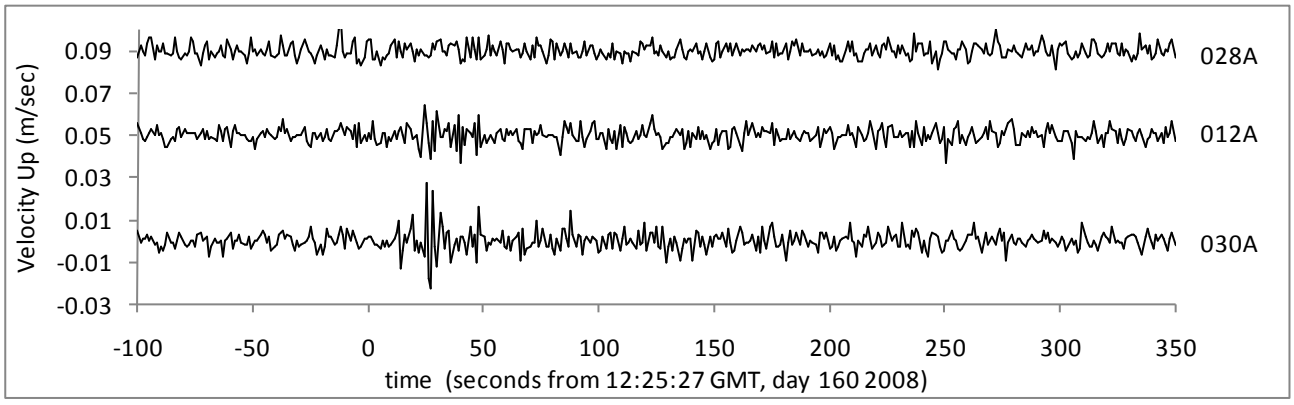

Fig. 6. Time-series (12:23 - 12:31) of velocity (Up component) obtained from the PPP solution.

4.2 Baseline results

The analysis of the PPP solutions showed that among the five stations investigated, station 001A is the only one that can be considered unaffected by the earthquake, or at least any possible motion at 001A is below the noise level of the estimated positions and velocities. For this reason 001A has been chosen as base station for the computation of the baseline solutions.

Fig. 7 shows the time-series of East of stations 030A and 012A as computed from the kinematic solution of the baselines 001A-030A and 001A-012A, respectively. The entire 1-hour interval is displayed in the figure, so that the baseline results can be compared to the PPP approach regarding the variability of the solution. Observing Fig. 7 and Fig. 3, it can be concluded that both solutions are adequate for the detection of the displacements. Fig. 8 gives a detailed view of the time-series of East and North a few minutes before and after the event. Comparing Fig. 8 to Fig. 4 it becomes obvious that the patterns of the displacements obtained from the two solutions are very similar. The same comes out for the estimated velocities if we compare Fig. 9 and Fig. 5. Regarding the

estimation of vertical motions we can compare the PPP and the baseline solutions only for the case of station 030A as it is the only station for which vertical movements have been verified (compare Fig. 10 and Fig. 6).

A comprehensive comparison between the PPP and baseline solutions is made in Tables 1 and 2. Table 1 gives the East and North dynamic displacements (peak to peak values) estimated by the two solutions and Table 2 gives the velocities. Dashes are used in cases it was not possible to detect any seismically-induced motion at a station. As can be seen in Tables 1 and 2 the two processing approaches yield very similar results. Only in the case of vertical motions at station 030A the PPP solution proved to be better as the motions were not detectable in the baseline results (Table 1). In general, the PPP Up estimates showed about 50% lower noise with respect to the baseline solutions. Regarding the East-North estimates the two approaches offer the same level of precision.

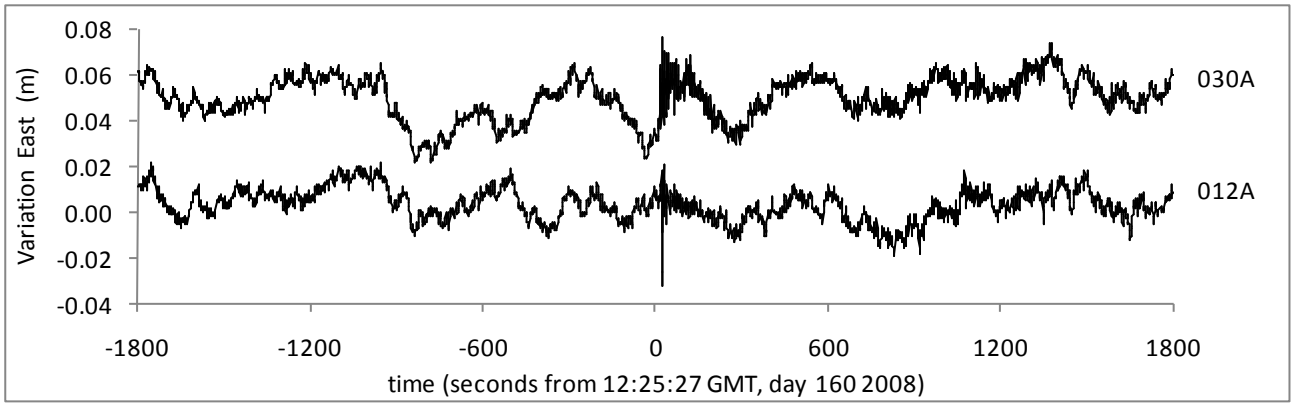

Fig. 7. Time-series (11:55 - 12:55) of East of stations 030A and 012A estimated by the baseline solutions.

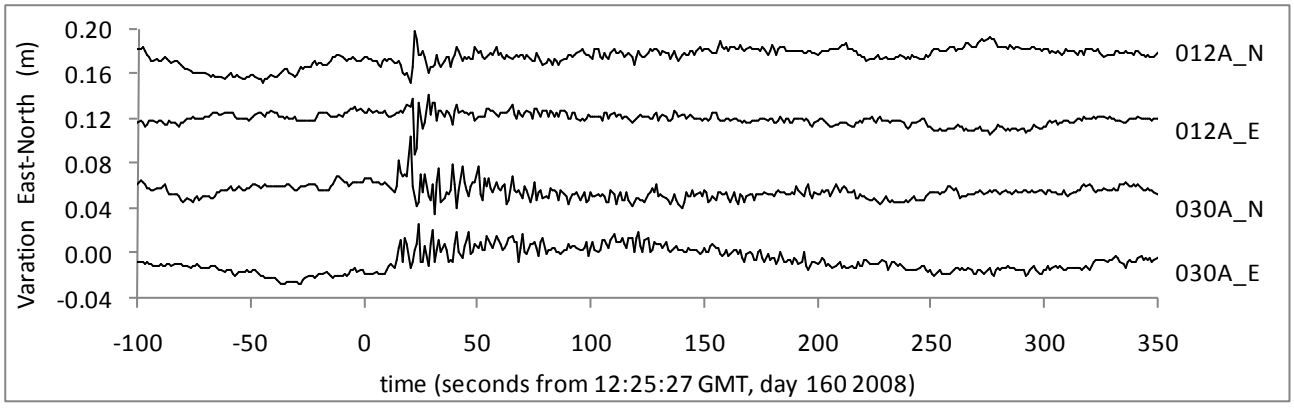

Fig. 8. Time-series (12:23 - 12:31) of East and North of stations 030A and 012A estimated by the baseline solutions.

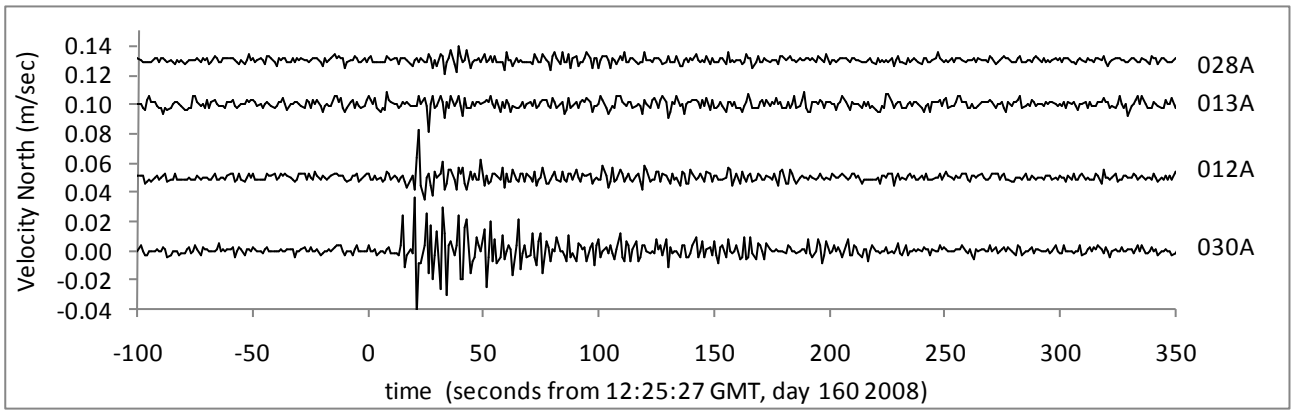

Fig. 9. Time-series (12:23 - 12:31) of stations' velocities (North component) estimated by the baseline solutions.

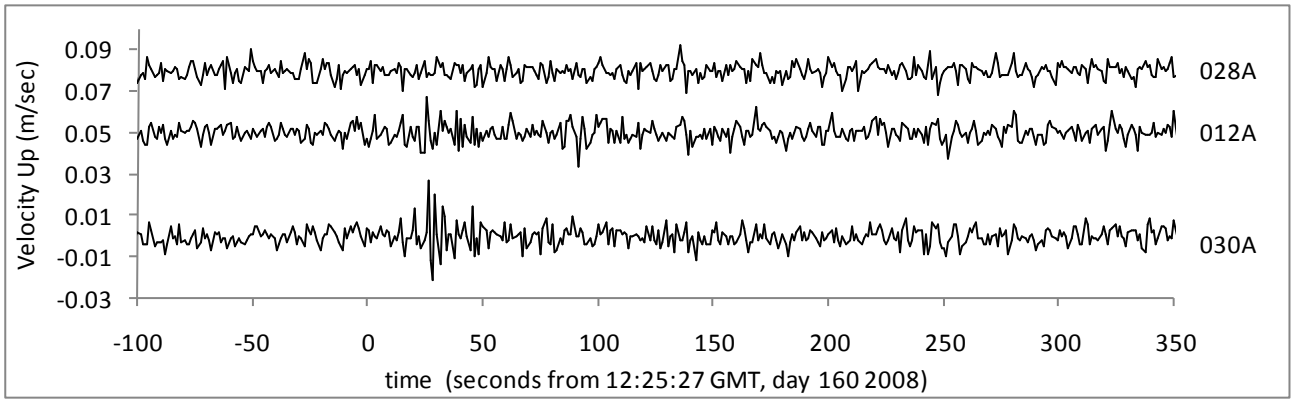

Fig. 10. Time-series (12:23 - 12:31) of velocity (Up component) obtained from the baseline solutions.

Table 1. East-North-Up displacements (mm) during the event (peak to peak values) as estimated from the PPP and the baseline solutions.

	030A			**012A**			**013A**			**028A**		
	E	**N**	**U**	**E**	**N**	**U**	**E**	**N**	**U**	**E**	**N**	**U**
PPP solution	47	67	42	56	47	-	-	-	-	-	-	-
Baseline solution	40	69	-	53	46	-	-	-	-	-	-	-

Table 2. East-North-Up velocities (mm/sec) during the event (peak to peak values) as estimated from the PPP and the baseline solutions.

	030A			**012A**			**013A**			**028A**		
	E	**N**	**U**	**E**	**N**	**U**	**E**	**N**	**U**	**E**	**N**	**U**
PPP solution	58	82	50	94	44	27	12	28	-	9	20	-
Baseline solution	57	79	48	91	47	23	12	25	-	11	19	-

5. Discussion

The arrival of the surface seismic waves of the Andravida earthquake has been observed using coordinate time-series produced from both PPP and baseline solutions. It has been shown that the station velocity is more adequate for determining the arrival of the seismic waves and the duration of the co-seismic displacements. Unlike the coordinates that suffer from periodic variations, the velocity remains close to zero as long as the station is not in motion, so any changes can be easily detected. This fact can be exploited for the detection of seismic ground motions in a real-time environment using an automated procedure.

Peak-to-peak motions exceeding 6 cm have been revealed using both PPP and baseline solutions. Before using these results for seismological purposes three aspects should be considered, namely the sampling rate of the GPS data, the processing algorithms and the antenna monumentation. The data used were sampled at 1 sec, which is not sufficient to provide "alias-free" solutions of co-seismic dynamic displacements (Avallone et al., 2011). The epoch solutions obtained using Kalman filter algorithms are always correlated, as each state vector is computed taking into account the state vector of the previous epoch. Thus, the arrival of the seismic waves may appear with a small time lag. Lastly, the most critical aspect that influences the results is the antenna monumentation. All HEPOS stations are installed on buildings using rigid steel masts that are 10 cm in diameter. The length of the mast between the highest anchorage and the antenna is about 1.3 m in the case of roof-

mounted antennas and about 2 m in the case of side-mounted antennas. Thus, the resonant frequency of the system building-mast significantly influences the dynamic behavior of the GPS antenna during an earthquake.

6. Conclusions

In this study we tested kinematic baseline and PPP solutions for the detection of seismically-induced surface motion. The Andravida earthquake (Mw 6.4) was used as case study. We computed velocities from the coordinate time-series. The velocities proved to be more appropriate than the coordinates for detecting the arrival time of the seismic wave. Moreover, the velocities are useful for the estimation of the duration of the dynamic displacements at each station.

Regarding the estimation of the displacements' amplitude, the PPP and the baseline approaches complement each other. Short-baselines solutions show lower noise than PPP solutions, but are yielding relative displacements, as in the general case the base station suffers also from deformations due to the seismic waves. On the contrary, PPP solutions offer directly absolute displacements.

RTK-networks like HEPOS offer the possibility to estimate the arrival time of the seismic waves at several stations in different directions and at different distances from the epicenter. Of course, for the interpretation of the estimated amplitude and duration of the displacements we should keep in mind that in most RTK networks the antennas are mounted on buildings using steel masts which exaggerate the motion.

Acknowledgments

The HEPOS project was co-funded by the European Regional Development Fund in the framework of the Operational Program "Information Society". Useful discussions with Dimitrios Mastoris, Head of Geodetic Department of NCMA S.A., are warmly acknowledged.

References

Avallone, A., Marzario, M., Cirella, A., et al. Very high rate (10 Hz) GPS seismology for moderate-magnitude earthquakes: The case of the Mw 6.3 L'Aquila (central Italy) event. J. Geophys. Res. 116, art. B02305, 2011.

Bock, Y., Nikolaidis, R. M., de Jonge, P. J., et al. Instantaneous geodetic positioning at medium distances with the Global Positioning System. J. Geophys. Res. 105, 28,233– 28,253, 2000.

Ganas, A., Serpelloni, E., Drakatos, G.,et al. The Mw 6.4 SW-Achaia (western Greece) Earthquake of 8 June 2008: seismological, Field, GPS Observations, and Stress Modeling. J. Earth. Eng.. 13, 1101-1124, 2008.

Genrich, J. F., Bock, Y. Rapid resolution of crustal motion at short ranges with the Global Positioning System. J. Geophys. Res. 97, 3261-3269, 1992.

Gianniou, M. Tectonic deformations in Greece and the operation of HEPOS network. EUREF 2010 Symposium Gävle, Sweden. June 2-4, 2010a.

Gianniou, M. Investigating the Effects of Earthquakes Using HEPOS, in: Mertikas S.P. (Ed.), Gravity, Geoid and Earth Observation, IAG Symp., 135, Springer Verlag, pp. 661-668, 2010b.

Herring, T. A., King, R. W., McClusky, S. C,. GAMIT Reference Manual GPS Analysis at MIT, Release 10.4. Cambridge: Massachusetts Institute of Technology, 2010.

Hollenstein, C. GPS deformation field and geodynamic implications for the Hellenic plate boundary region. Swiss Federal Institute of Technology Zurich, Diss. ETH. 16593, 2006.

Kouba, J. A Guide to using International GPS Service (IGS) products. http://igscb.jpl.nasa.gov/igscb/resource/pubs/GuidetoUsingIGSProducts.pdf, 2003a.

Kouba, J. Measuring seismic waves induced by large earthquakes with GPS. Stud. Geophys. Geod. 47(4), 741–755, 2003b.

Margaris, B., Papaioannou, C., Theodoulidis, N. et al. Preliminary report on the principal seismological and engineering aspects of the Mw = 6.5 Achaia-Ilia (Greece) earthquake on 8 June 2008. Report of the Geotechnical Earthquake Engineering Reconnaissance (GEER) Team, GEER Association Report No. GEER-013, 2008.

Nikolaidis, R. M., Bock, Y., de Jonge, P. J., et al. Seismic wave observations with the Global Positioning System. J. Geophys. Res. 106, 21,897-21,916, 2001.

Novatel. GrafNav / GrafNet User Guide. http://www.novatel.com/assets/Documents/Waypoint/Downloads/NavNet840_Manual.pdf, 2011.

Novatel. Static Precise Point Positioning Accuracy in GrafNav 8.10. http://www.novatel.com/assets/Documents/Waypoint/Reports/StaticPPP.pdf, 2008.

Takasu, T. High-rate Precise Point Positioning: Detection of crustal deformation by using 1-Hz GPS data. GPS/GNSS Symposium 2006, Tokyo, 2006.

Yusaku, O., Ohzono, M., Miura, S., et al. Coseismic fault model of the 2008 Iwate-Miyagi Nairiku earthquake deduced by a dense GPS network. Earth Planets Space, 60, 1197–1201, 2008.